Wu *et al. Geoscience Letters* (2023) 10:59
https://doi.org/10.1186/s40562-023-00314-6

Geoscience Letters

RESEARCH LETTER

Open Access

Magnitude determination using cumulative absolute absement for earthquake early warning

Yih-Min Wu[1,2,3*], Himanshu Mittal[4], Yueh-Ho Lin[1] and Yu-Hsuan Chang[1]

Abstract

The cumulative absolute absement (CAA) of the 3 s window after P-wave arrival can be used to estimate the magnitude (M_{CAA}) of an earthquake. This method can achieve good results even when only the six stations nearest to the epicenter are used. The standard deviation between the estimated CAA magnitude (M_{CAA}) and the moment magnitude (M_w) is found to be 0.3 when using either 6 or 20 stations. This means that M_{CAA} can be reliably predicted using the closest 6 stations. On the other hand, the magnitude (M_{Pd}) derived from P_d using the closest 20 stations has a standard deviation of 0.4 between the estimated M_{Pd} and M_w. This suggests that CAA is a better magnitude determination parameter for the EEW system than P_d.

Keywords Earthquake, Early Warning, P-waves, Magnitude

Introduction

Earthquake Early Warning (EEW) systems play a crucial role in providing advance alerts before the arrival of strong ground shaking following a destructive earthquake. These systems send out alerts within a few seconds, enabling people to take immediate action and save lives before the arrival of damaging S-waves. On-site EEW relies on the initial P-wave signals from a single station or a small array to rapidly determine the intensity of the destructive S-waves. Regional EEW systems, on the other hand, utilize seismic data from multiple stations near the epicenter to estimate the earthquake's intensity, location, and magnitude. Regional EEW systems offer greater accuracy compared to on-site EEW. One of the key challenges in EEW is the quick and accurate estimation of earthquake magnitude using the early seismic signals (P-waves) recorded by a limited number of stations close to the epicenter (Mittal et al. 2022). Traditional approaches involve analyzing the amplitude and frequency (period) parameters of the initial P-waves for this purpose (Nakamura 1988; Kanamori 2005; Wu and Zhao 2006). Noteworthy period parameters for rapid magnitude estimation include the average period (τ_c) and the maximum dominant ground motion period (τ_p^{max}). These period parameters are employed because the frequency information conveyed by the initial seconds of P-waves exhibits high sensitivity to the final magnitude while being less affected by the attenuation of seismic waves over distance (Nakamura 1988; Wu and Kanamori 2005a; Wu et al. 2007; Allen and Kanamori 2003; Yamada and Mori 2009; Zollo et al. 2010).

Studies have shown that τ_c tends to increase with earthquake size and displays less saturation (Kanamori 2005). However, it should be noted that τ_c is susceptible to background noise and the rupture process, which can sometimes lead to inaccuracies in magnitude estimation

*Correspondence:
Yih-Min Wu
drymwu@g.ntu.edu.tw; drymwu@ntu.edu.tw
[1] Department of Geosciences, National Taiwan University, No. 1, Section 4, Roosevelt Road, Taipei 10617, Taiwan
[2] Institute of Earth Sciences, Academia Sinica, Taipei 11529, Taiwan
[3] Research Center for Future Earth, National Taiwan University, Taipei 10617, Taiwan
[4] National Centre for Seismology, Ministry of Earth Sciences, New Delhi 110003, India

(Yamada and Mori 2009; Ziv 2014). Researchers have extensively explored the use of these period parameters for magnitude estimation due to their valuable frequency information and robustness against distance-dependent wave attenuation (Nakamura 1988; Wu and Kanamori 2005a; Wu et al. 2007; Allen and Kanamori 2003; Yamada and Mori 2009; Zollo et al. 2010).

The magnitude of an earthquake can be estimated by analyzing the peak vertical displacement (P_d) observed in the initial seconds after the arrival of the P-wave. Previous studies conducted by Wu and Zhao (2006) have demonstrated a strong correlation between the estimated P_d, obtained from a 3 s window following the P-wave arrival, and the magnitude estimate (M_{Pd}). Peak ground velocity (PGV) is considered a reliable indicator of earthquake intensity, and it can be estimated from P_d using a regression relationship established by Wu and Kanamori (2005b, 2008a, 2008b). The magnitude calculations based on period parameters generally exhibit larger uncertainties compared to amplitude parameters. However, amplitude parameters also suffer from magnitude saturation issues for larger events (Wu et al. 2006; Hoshiba and Iwakiri 2011). Therefore, considering both amplitude and frequency parameters together is deemed effective for EEW, as highlighted in the work of Hsiao et al. (2009).

Another category of EEW parameters used for magnitude estimation is cumulative absolute velocity (CAV), which is based on integral measurements. Initially introduced by the Electrical Power Research Institute (EPRI 1988) to assess potentially damaging earthquakes for nuclear power plants, the definition of CAV has been refined by seismologists over time (e.g., EPRI 1991; Wu and Teng 2004; Kramer and Mitchell 2006) for use with ground motion prediction equations and EEW systems. Successful applications of CAV in the Istanbul EEW system were reported by Erdik et al. (2003). Furthermore, logarithmic CAV calculations have shown good agreement with magnitude (Bose et al. 2008; Alcik et al. 2009). Various mathematical definitions of CAV parameters exist for different usage scenarios.

In prior study, Wu and Kanamori (2005a, b) compared the peak amplitudes of acceleration, velocity, and displacement of the initial P-waves for EEW applications. It was discerned that the P_d exhibited superior performance. Subsequently, Wu and Zhao (2006) leveraged P_d for magnitude determination in the EEW system, an approach that has since been adopted widely (Zollo et al. 2006). Generally, displacement is more effective in capturing low-frequency information compared to velocity and acceleration. However, P_d has its limitations; it only captures the peak value of the initial P-waves, offering no additional insight. In contrast, CAV, as defined by EPRI (1988), provides a more encompassing perspective by integrating the absolute value of acceleration, surpassing mere peak values. Consequently, we explored CAA for our EEW system, a derivative of the integrals of absolute values of velocity and displacement, termed cumulative absolute displacement (CAD) and absement, respectively.

The subsequent studies (Huang and Wu 2021; Chang and Wu 2022) compared CAV, CAD, CAA, P_d, and τ_c for magnitude estimation. The initial CAA demonstrated a stronger correlation with magnitude compared to other parameters. The magnitude saturation may still persist even when utilizing the CAA. These findings motivate further exploration of estimating earthquake magnitude based on the initial CAA and investigating the discrepancies between magnitude estimates derived from CAA and P_d.

Data and analysis

This study makes use of 1520 K-net strong motion records from 76 events with moment magnitudes ranging from 5.5 to 8.3. The earthquakes that occurred within the area enclosed by 30–46° N and 129–147° E from January 1996 to May 2021 are selected (Fig. 1a). The K-net strong motion network is operated by the National Research Institute for Earth Science and Disaster Resilience (NIED) in Japan. The network, which consists of over 1,000 seismometers distributed around Japan, is intended to measure severe ground motion during earthquakes. The shallow-depth earthquakes are selected for the present study. The data are selected based on two criteria. Firstly, the earthquakes are selected with $M_w \geq 5.5$, focal depth ≤ 30 km. To ensure enough station coverage and prevent P-wave contamination due to the path effect over a great distance, the screening condition of recording at 10 stations within 50 km from the epicenter is applied. This criterion, however, excludes large-magnitude earthquakes off the coast of Japan and includes moderate-magnitude inland earthquakes with magnitudes ranging from 5.5 to 6.4. To include the high-magnitude earthquakes, a second screening criterion is applied. In the second condition, the earthquakes with $M_w \geq 6.5$, focal depth ≤ 50 km, and have recorded at 20 stations within a radius of 200 km are selected (Fig. 1b). For every earthquake, only the nearest 20 records are used for analysis.

After removing the average from the original three-component acceleration waveform, the vertical component of the acceleration record was subjected to Allen's (1978) automatic wave picking method based on the ratio of the short-time window signal average value to the long-time window signal average value. Considering that some earthquake sequences are relatively complex, the seismic waveforms of the mainshock and aftershock may be captured in the same earthquake trace, which will cause an error in the automatically picked P-wave arrival.

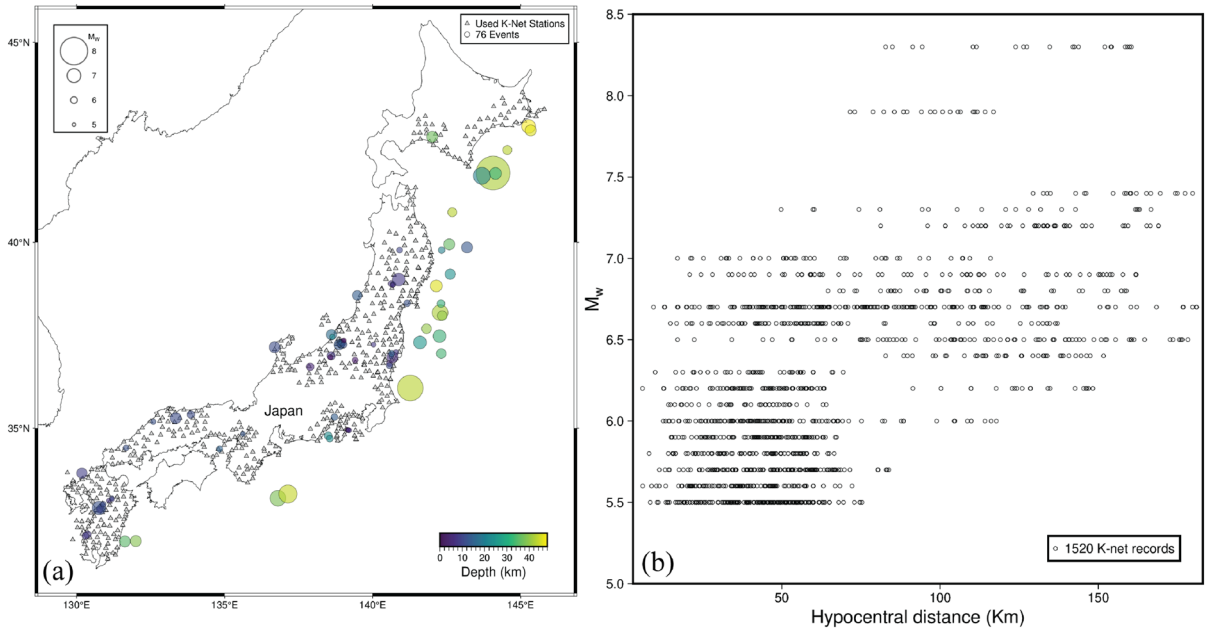

Fig. 1 **a** The location of the instruments used in the present study. **b** The distribution of earthquake magnitude with hypocentral distance

For the events where the automated picked time does not match the time of the earthquake (with an allowable difference of ± 0.5 s), the records are removed manually for the picking of P-wave arrival.

Following details by Wu and Teng (2004), CAA is defined as

$$CAA = \int_{T_p}^{T_{p+i}} \sqrt{Dv^2 + Dn^2 + De^2}\,dt, \quad (1)$$

where Dv, Dn, and De stand for the vertical, north–south, and east–west displacement amplitudes, respectively. p labels the arrival of the P-waves, and i designates the time interval that follows.

P_d is simply the peak value from the vertical displacement after the arrival of the P-waves. Once the CAA and P_d are estimated, M_{CAA} and M_{Pd} are estimated using the following regression:

$$Log(P_d) = a * \log(R) + b * M_w + c, \quad (2)$$

$$Log(CAA) = a * \log(R) + b * M_w + c, \quad (3)$$

where R is the hypocentral distance in km.

Results

Getting a reliable earthquake location and magnitude quickly in the early stages of an earthquake is an essential challenge in EEW. It is extremely straightforward to rapidly report the earthquake location using the usual traditional travel time method. However, immediate and accurate earthquake magnitude estimation remains an urgent concern in EEW research, particularly for large earthquakes.

CAA and P_d estimation

In Fig. 2, the distribution of P_d and CAA is presented for different hypocentral distances. It can be observed that, across all earthquake magnitudes, the P_d values are consistently lower than the corresponding CAA values (although CAA and P_d represent distinct parameters, a comparison is performed to identify the magnitude threshold using the two). Higher magnitude earthquakes (≥ 7.0) are recorded at distances beyond 50 km from the hypocenter. Within a 50 km range, earthquakes with magnitudes between 5.0 and 7.0 are observed, and both CAA and P_d values decrease as the hypocentral distance increases. Notably, there is a larger variation in P_d values compared to CAA values.

In the case of P_d values for fitting the trend, a significant number of outliers have been identified across different magnitude ranges. This suggests that P_d values can exhibit substantial variability and may not always follow a consistent pattern with respect to earthquake magnitude. Conversely, when examining CAA values, we have observed a consistent and constant decrease as hypocentral distance increases. This means that, irrespective of earthquake magnitude, CAA values tend to exhibit a predictable decrease with distance from the earthquake source. This behavior suggests that CAA values are less susceptible to the influence of outliers and follow a more

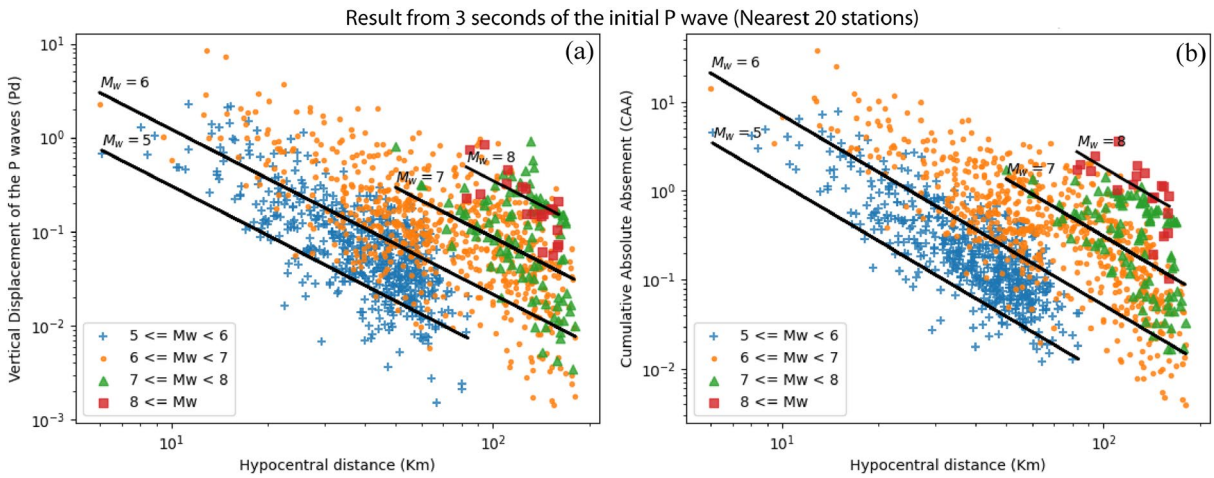

Fig. 2 The variation of P_d (**a**) and CAA (**b**) with hypocentral distance for a 3 s window

regular pattern, making them a more stable parameter in EEW, particularly when assessing the cumulative displacement experienced at varying distances from the source.

Magnitude estimation using P_d

To determine the optimal empirical relationship for large-magnitude earthquakes in Japan using the P_d parameter from a 3 s window, a dataset comprising 1520 earthquake records from 76 earthquake events is analyzed. The estimation of M_{Pd} is initially compared with M_{CAA}. In previous studies, P_d is defined as the maximum vertical absolute displacement within three seconds following the arrival of the P-wave. Although the value of P_d remains relatively stable within the 3 s window, Huang and Wu (2021) demonstrated that P_d increases as the time window after the P-wave arrival expands, reaching its maximum amplitude. This maximum amplitude is not limited to the 3 s time window.

Table 1 presents the estimation of M_{Pd} using the closest 20 stations, considering five different windows with a 1 s interval. The analysis reveals that when utilizing these 20 stations, the variation between the estimated and actual magnitude is approximately ± 0.43 within the 3 s window (Fig. 3a).

Magnitude estimation using CAA

The displacement amplitudes of the three seismic components are integrated in the time domain after the P-wave arrival to obtain the CAA values. For each seismic record, CAA is calculated using five different window lengths at 1 s intervals following the P-wave arrival. Regression analysis is then conducted using all 76 earthquakes, employing the least square method for different window lengths. The M_{CAA} values for each earthquake are determined by averaging the values from the corresponding stations.

Considering that distant records may experience lower energy and potential contamination from surrounding

Table 1 The values of constants in Eqs. (2) and (3) and the relation between M_{CAA} and actual M_w, M_{pd}, and actual M_w for different time windows using 20 stations

Parameter	Window(s)	Stations	a	b	c	SDE	Magnitude
P_d	1	20	−1.620	0.637	−2.573	0.477	M_w=M_{pd} ±0.40
	2		−1.687	0.584	−1.898	0.437	M_w=M_{pd} ±0.42
	3		−1.749	0.603	−1.780	0.413	M_w=M_{pd} ±0.43
	4		−1.807	0.635	−1.771	0.391	M_w=M_{pd} ±0.42
	5		−1.901	0.682	−1.820	0.368	M_w=M_{pd} ±0.37
CAA	1	20	−1.995	0.761	−2.408	0.407	M_w=M_{CAA} ±0.31
	2		−2.059	0.778	−2.057	0.389	M_w=M_{CAA} ±0.31
	3		−2.132	0.773	−1.658	0.373	M_w=M_{CAA} ±0.34
	4		−2.181	0.764	−1.326	0.360	M_w=M_{CAA} ±0.34
	5		−2.227	0.756	−1.049	0.342	M_w=M_{CAA} ±0.33

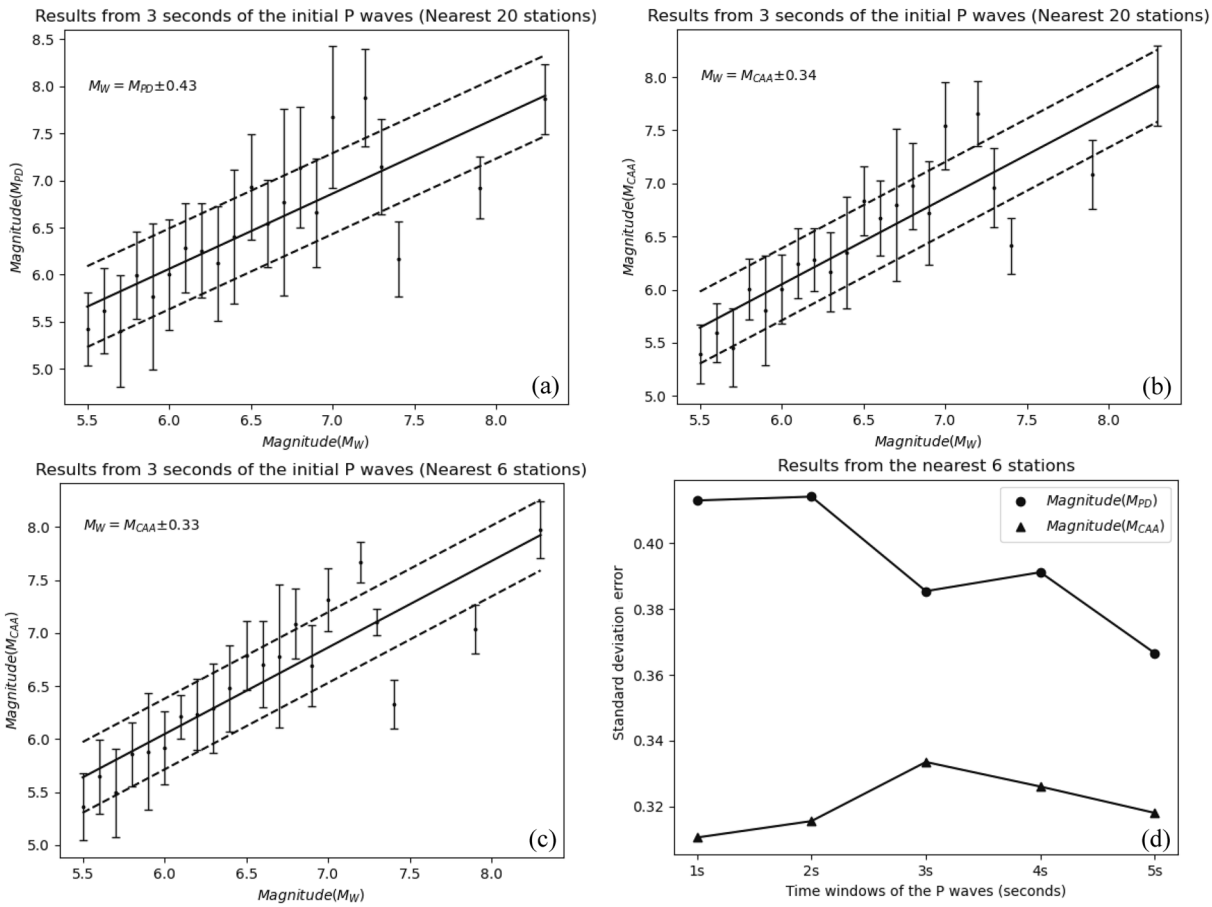

Fig. 3 **a** The variation between M_w and M_{Pd} using the nearest 20 stations in the 3 s window, **b** The variation between M_w and M_{CAA} using the nearest 20 stations in the 3 s window, **c** using the nearest 6 stations, **d** the standard deviation error for M_{Pd} and M_{CAA} for different time windows using 6 stations

noise, it is essential to strike a balance between data accuracy and warning time. This study emphasizes the significance of estimating magnitude using a reduced number of stations close to the epicenter. To assess the accuracy, a comparison is made using data from the nearest six and twenty stations relative to the epicenter. The comparison is based on the standard deviation error (SDE).

Estimated magnitude and M_w—Analysis results using records of 76 earthquakes

Using 20 stations of 76 earthquakes, the coefficients and constants corresponding to each parameter item in Eqs. (1) and (2) under 5-time windows were obtained through least squares regression (Table 1). The variations between the M_{CAA} of the 76 earthquakes and the M_w are shown in Table 1, which are used as a reference for the accuracy of the estimation results.

The results showed that under the 5-time windows, the standard deviation error reached a statistically low value with an increase in the time window. Based on the comparison charts of SDE in Table 1, it can be seen that there are some differences in the values under each time window as a whole. By comparing the estimated magnitudes derived from P_d and CAA with the moment magnitude, some variations are observed between the two magnitude estimates for 1 s and 2 s windows. With the increase in window length to 3 s, these variations become more consistent, measuring at approximately ± 0.42 for P_d and ± 0.34 for CAA. Only in the initial 3 s window, the SDE value is smaller. Further increasing the window length to 5 s results in SDE reducing to ± 0.34 for P_d and ± 0.33 for CAA. The deviation in estimated magnitude and M_w, based on the initial 3 s of data following the arrival of P-waves, is approximately 0.34, which is within the acceptable range of ± 0.3 in EEW systems. This means that the magnitude estimated using CAA can provide a better magnitude estimation.

Figure 3b and Fig. 3c show the comparison of estimated M_{CAA} using the closest 20 stations and 6 stations in the initial 3 s window. In Fig. 3d, the depicted SDE

corresponds to the comparison of the two estimated magnitudes with the moment magnitude, using data from six stations. Across different window lengths, the SDE for the P_d magnitude varies between 0.42 and 0.37, while for CAA, it exhibits a narrower range, spanning from 0.29 to 0.33. In terms of SDE, obtained results using 20 stations are not better than the results obtained by using only 6 stations. The key point is that the SDE using 20 stations of 76 earthquakes is not lower than the standard deviation calculated at 6 stations with closer epicentral distances in the initial 3 s window. Generally, more stations close to the epicenter will produce reliable results but at the cost of reduced warning time (Yang et al.2021). However, looking at the present analysis, the results presented using 6 stations in the initial 3 s window provide a reasonable magnitude analysis and may be helpful as maximum warning time can be achieved.

Discussion and conclusions

This study examines the strong ground motion records of medium and large-magnitude earthquakes obtained from NIED K-NET. The analysis focuses on two ground motion parameters: CAA and P_d. The study demonstrates the effectiveness of using the CAA parameter directly for magnitude estimation, specifically for earthquakes with depths less than 50 km in Japan. All three components (vertical, horizontal NS, and horizontal EW) and various time windows following the P-wave arrival were considered in the analysis. While CAA offers some advantages, it is essential to recognize that both CAA and CAV have their specific applications and may be chosen based on the particular needs of a given study or analysis. The preference for one over the other depends on the context, data quality, and the specific objectives of the analysis. In some cases, it may be beneficial to utilize both CAA and CAV to gain a more comprehensive understanding of ground motion characteristics. CAA captures low-frequency information more effectively than CAV. This can be important for assessing structural damage or deformation caused by long-duration ground motion. CAA provides insights into the energy content of ground motion, which can be valuable for assessing structural response and potential damage. For EEW systems and post-event assessment, CAA can help in assessing the actual displacement levels experienced by structures, aiding in the development of effective mitigation and response strategies.

The results indicate that employing a larger time window allows for the inclusion of the S-wave portion in the analysis. However, despite this inclusion, the calculated magnitude remains in good agreement with M_w. While using a longer time window may lead to improved magnitude estimation, it comes at the expense of reduced warning time. In this study, CAA was utilized for magnitude estimation and compared to P_d. It was found that CAA outperforms P_d even when using data from the nearest six stations. As the time window increases, the standard deviation of M_{Pd} (magnitude estimation using P_d) demonstrates a decreasing trend. On the other hand, the standard deviation of M_{CAA} (magnitude estimation using CAA) ranges from 0.31 to 0.33 for different time windows ranging from 1 to 5 s, with no significant trend observed as the window length increases (Fig. 3d). Based on the above results, the conclusions are summarized as follows:

1. Using 20 stations, the standard deviation error for M_{CAA} changes from 0.34 to 0.31 within different window lengths ranging from 1 to 5 s after the arrival of the P-wave. The magnitude error between the predicted and actual magnitude is close to an acceptable range of ± 0.3 in EEW operation.
2. Similarly, using 6 stations for M_{CAA} estimation, the SDE improves from 0.31 to 0.33 within different window lengths ranging from 1 to 5 s. The variation in magnitude estimation using the nearest 6 stations close to the epicenter in the initial 3 s window is similar to using 20 stations, i.e., 0.33, but the results hold promising in terms of improvement in standard deviation error.
3. The estimated magnitude using P_d shows a high variation between the predicted and M_w in comparison to CAA. The variation in magnitude ranges from ± 0.43 to ± 0.37. For the 3 s window, the variation is in the order of ± 0.43.

By comparing the estimated earthquake magnitude using CAA and P_d, it is found that CAA can be added as a better magnitude estimation parameter in the future earthquake early warning system. However, the magnitude saturation may still exist and need to be explored in future studies.

Abbreviations

CAA	Cumulative absolute absement
EEW	Earthquake early warning
P_d	Peak vertical displacement
PGV	Peak ground velocity
CAV	Cumulative absolute velocity
EPRI	Electrical Power Research Institute
CAD	Cumulative Absolute Displacement
NIED	National Research Institute for Earth Science and Disaster Resilience
SDE	Standard deviation error

Acknowledgements

The authors gratefully acknowledge the National Science and Technology Council (NSTC), Taiwan for sponsoring the project. They would like to thank National Research Institute for Earth Science and Disaster Resilience (NIED) in

Japan for providing K-net strong motion records. The author, HM, is grateful to the Director, NCS-MoES, India for his permission to participate in this study

Author contributions
YMW contributed to conceptualization; YMW and YHC contributed to methodology; YHL and YHC provided software and were involved in formal analysis; YMW and HM were responsible for validation, writing—original draft preparation, and writing—review and editing; YMW, HM, YHL, and YHC were involved in investigation; YMW provided resources and performed supervision, project administration, and funding acquisition; YMW, YHL, and YHC were involved in data curation; YHL contributed to visualization. All authors have read and agreed to the published version of the manuscript. All authors contributed to all sections until the final revision of the manuscripts.

Funding
This study was supported by the National Science and Technology Council, Taiwan, with Grant Numbers 111-2116-M002-031 and 109-2116-M-002-030-MY3.

Availability of data and materials
The strong motion waveform records from the K-net network used in this study can be downloaded at https://www.kyoshin.bosai.go.jp/.

Declarations

Ethics approval and consent to participate
Not applicable.

Consent for publication
Not applicable.

Competing Interests
The authors declare no conflict of interest.

Received: 13 July 2023 Accepted: 30 November 2023
Published online: 11 December 2023

References

Alcik H, Ozel O, Apaydin N, Erdik M (2009) A Study on Warning Algorithms for Istanbul Earthquake Early Warning System. Geophys Res Lett 36:L00B05
Allen RV (1978) Automatic earthquake recognition and timing from single traces. Bull Seismol Soc Am 68:1521–1532
Allen RM, Kanamori H (2003) The potential for earthquake early warning in southern California. Science 300(5620):786–789
Böse M, Wenzel F, Erdik M (2008) PreSEIS: a neural network-based approach to earthquake early warning for finite FaultsPreSEIS: A neural network-based approach to earthquake early warning for finite faults. Bull Seismol Soc Am 98(1):366–382
Chang YH, Wu YM (2022) Fast magnitude estimation for Mw ≥ 5.5 earthquakes in Japan, Taiwan Geosciences Assembly, June 7–10, 2022, Taipei, Taiwan.
EPRI (1988). A criterion for determining exceedance of the operating basis earthquake, Electric Power Research Institute, Palo Alto, CA, prepared by Jack R. Benjamin and Associates, inc., Report No:NP-5930.
EPRI (1991). Standardization of the cumulative absolute velocity. In: Electric Power Research Institute, Palo Alto, CA, prepared by Yanke Atomic Electric Company, Report No:TR-100082.
Erdik M, Fahjan Y, Ozel O, Alcik H, Mert A, Gul M (2003) Istanbul earthquake rapid response and the early warning system. Bull Earthq Eng 1:157–163. https://doi.org/10.1023/A:1024813612271
Hoshiba M, Iwakiri K (2011) Initial 30 seconds of the 2011 off the pacific coast of Tohoku Earthquake (Mw 9.0) -amplitude and τ_c for magnitude estimation for Earthquake Early Warning. Earth Planets Space 63:553–557
Hsiao NC, Wu YM, Shin TC, Zhao L, Teng TL (2009) Development of earthquake early warning system in Taiwan. Geophys Res Lett 36:02
Huang HY, Wu YM (2021) Magnitude Estimation and Onsite Earthquake Early Warning using Cumulative Absolute Velocity in Taiwan, EGU General Assembly 2021, online, 19–30 Apr 2021, EGU21-8570. https://doi.org/10.5194/egusphere-egu21-8570.
Kanamori H (2005) Real-time seismology and earthquake damage mitigation. Annu Rev Earth Planet Sci 33:195–214
Kramer SL, Mitchell RA (2006) Ground motion intensity measures for liquefaction hazard evaluation. Earthq Spectra 22(2):413–438
Mittal H, Yang BM, Wu YM (2022) Progress on the earthquake early warning and shakemaps system using low-cost sensors in Taiwan. Geoscience Letters 9:42. https://doi.org/10.1186/s40562-022-00251-w
Nakamura Y. (1988) On the urgent earthquake detection and alarm system. In: Proceedings of the 9th World Conference on Earthquake Engineering 7:673–678.
Wu YM, Kanamori H (2005a) Rapid assessment of damage potential of earthquakes in Taiwan from the beginning of P waves. Bull Seismol Soc Am 95(3):1181–1185
Wu YM, Kanamori H (2005b) Experiment on an onsite early warning method for the Taiwan early warning system. Bull Seismol Soc Am 95(1):347–353
Wu YM, Kanamori H (2008a) Exploring the feasibility of on-site earthquake early warning using close-in records of the 2007 Noto Hanto earthquake. Earth Planets Space 60(2):155–160
Wu YM, Kanamori H (2008b) Development of an earthquake early warning system using real-time strong motion signals. Sensors 8(1):1–9
Wu YM, Teng TL (2004) Near real-time magnitude determination for large crustal earthquakes. Tectonophysics 390(1–4):205–216
Wu YM, Zhao L (2006) Magnitude estimation using the first three seconds P-wave amplitude in earthquake early warning. Geophys Res Lett 33(16):L16312
Wu YM, Yen HY, Zhao L, Huang BS, Liang WT (2006) Magnitude determination using initial P waves: A single-station approach. Geophys Res Lett 33(5):L05306
Wu YM, Kanamori H, Allen RM, Hauksson E (2007) Determination of earthquake early warning parameters, τc and Pd, for southern California. Geophys J Int 170(2):711–717
Yamada M, Mori J (2009) Using τc to estimate magnitude for earthquake early warning and effects of near-field terms. J Geophys Res 114(B5):B05301
Yang BM, Mittal H, Wu YM (2021) Real-time production of PGA, PGV, Intensity, and Sa shakemaps using dense MEMS-based sensors in Taiwan. Sensors 21(3):943
Ziv A (2014) New frequency-based real-time magnitude proxy for earthquake early warning. Geophys Res Lett 41(20):7035–7040
Zollo A, Lancieri M, Nielsen S (2006) Earthquake magnitude estimation from peak amplitudes of very early seismic signals on strong motion. Geophys Res Lett 33(23):L23312. https://doi.org/10.1029/2006GL027795
Zollo A, Amoroso O, Lancieri M, Wu YM, Kanamori H (2010) A threshold-based earthquake early warning using dense accelerometer networks. Geophys J Int 183(2):963–974

Publisher's Note